

A Mini-Review of Shape-Memory Polymer-Based Materials

Stimuli-responsive shape-memory polymers

Mathew J. Haskew, John G. Hardy*

Department of Chemistry and Materials
Science Institute, Faraday Building, Lancaster
University, Lancaster, LA1 4YB, UK

*Email: j.g.hardy@lancaster.ac.uk

Shape-memory polymers (SMPs) enable the production of stimuli-responsive polymer-based materials with the ability to undergo a large recoverable deformation upon the application of an external stimulus. Academic and industrial research interest in the shape-memory effects (SMEs) of these SMP-based materials is growing for task-specific applications. This mini-review covers interesting aspects of SMP-based materials, their properties, how they may be investigated and highlights examples of the potential applications of these materials.

Introduction

SMEs refers to the ability of the material to memorise a shape and materials that possess these properties have a multitude of exciting technical and medical applications (1–14). For materials such as alloys this is commonly in a one-way SME (7, 15), however, there are a variety of materials that are capable of reverting to their permanent shape or original state upon exposure to a stimulus (such as a temperature change) or indeed multiple stimuli (16). SMP-based materials have been widely investigated since the 1980s because of the abundance of potential applications imparted by their interesting properties (for instance, stimuli-responsiveness and ability to change shape), which can lead to technological innovation and the generation of new high value products for technical and medical applications (1, 17–19).

The reversible transformation of SMPs functions by primary crosslinking net points (hard segments) memorising and determining the permanent shape, and secondary switching segments (soft segments) with a transition (T_{trans}) to reduce strain stress and hold the temporary shape. Below the T_{trans} , the material will be in its permanent shape and be stiffer than when T_{trans} is reached and the SMPs are more malleable and can be deformed into a desired shape (usually through application of an external force). The deformed state is maintained once the external force has been removed and the system is no longer at or above T_{trans} . SMPs revert to their original state once the T_{trans} conditions are met. This process describes the SME pathway of SMP-based materials that are thermally-induced (albeit not for some light or chemical-induced systems).

While most SMP-based materials hold a single permanent shape and a single temporary shape, recent advances in SMP technology have allowed the generation of multiple-shaped-memory materials with different stimuli responses (light or chemical) (16, 20, 21). An interesting example of this is a triple shaped-memory material generated by combining two dual SMPs with different glass transition temperatures (T_g) (22, 23), where the SMPs switch from one temporary shape to another at the first T_{trans} , and then back to the permanent shape at another, higher activation temperature (22).

SMPs have a large range of properties from stable to biodegradable and transient, elastic to rigid or soft to hard, depending on the structural units that constitute the SMP. Consequently, SMPs not only respond to temperature (24) and magnetism (25) like shape-memory alloys (SMAs) (26), but also to moisture (27), electricity (28), light (29) and chemical stimuli (such as a pH change) (30). Moreover, there are other principles of SME; for instance, a thermal-responsive SMP can proceed

via a Diels-Alder reaction (chemical crosslinking/reversible covalent bonds) (31). SMPs tend to have much milder processing conditions than SMAs (<200°C, low pressure), have a greater extent of deformation (strain more than 200% for most materials) and tend to be based on cheap starting materials with simple synthetic procedures (12, 32). After the term 'shape-memory' was first proposed by Vernon in 1941 (32), the significance of SMPs was not fully realised until the 1960s, when crosslinked polyethylene (PE) was used to make heat-shrinkable tubes and films (33). Significant investment in the development of SMPs began in the 1980s (34) with rapid progress realised in the last decade, particularly with a view to the generation of shape-memory materials with exciting and versatile features.

Shape-Memory Polymer Function

Two important quantities used to describe SMEs are the strain recovery rate (R_r) and the strain fixity rate (R_f). R_r describes the ability of a material to memorise its permanent shape, while R_f describes the ability of switching segments to fix the mechanical deformation. R_r is calculated using Equation (i):

$$R_r(N) = \frac{\varepsilon_m(N) - \varepsilon_p(N)}{\varepsilon_m(N) - \varepsilon_p(N-1)} \times 100\% \quad (i)$$

where N is the cycle number, ε_m is the maximum strain imposed on the material and ε_p is the strain of the sample after recovery. R_f is calculated using Equation (ii):

$$R_f(N) = \frac{\varepsilon_u(N)}{\varepsilon_m(N)} \times 100\% \quad (ii)$$

where ε_u is the strain in the fixed temporary shape. SMPs respond to specific stimuli through changes in their macroscopic properties (for example, shape) (26). The polymer network underlying active movement involves a dual system, one that is highly elastic and another that can reduce the stiffness upon application of a certain stimulus. The latter system incorporates either molecular switches or stimulus sensitive domains (35). Their shape-memory feature is a result of the combination of the polymer's architecture, and a programming procedure that enables the formation of a temporary shape. Net points consist of covalent bonds or intermolecular interactions and the SMP's

hard segments form the net points that link the soft segments (acting as a fixed phase), whereas the soft segments work as the molecular switches (acting as a reversible phase). The fixed phase prevents free flow of the surrounding polymer chains upon the application of stress. The reversible phase, on the other hand, undergoes deformation in a shape-memory cycle and is responsible for elasticity. For example, if the T_{trans} is T_g , the micro-Brownian motion of the network chains is fixed at low temperature (below T_g) and will be switched back on at high temperature (above T_g), recovering its original state. When T_{trans} is the crystal melting temperature (T_m), the switching segments crystallise at low temperature (below T_m), and then recover their original state at high temperature (above T_m). In addition, T_g normally extends over a broader temperature range compared to T_m , which tends to have relatively sharper transitions in most cases (26). Moreover, after the exposure to a specific stimulus and the T_{trans} is achieved, the strain energy in the deformed state is released, resulting in the shape recovery phenomenon. The general process of this SME for SMPs is depicted in **Figure 1**, wherein the polymer network structure is either chemically or physically crosslinked and the switching units are made from a semi-crystalline or amorphous phase.

Shape-memory behaviour can be demonstrated in various polymer systems that are significantly different in molecular structure and morphology. SME mechanisms differ according to the specific SMP(s); for instance, the SME mechanism of the chemically crosslinked semi-crystalline PE SMP. The crystalline phase, with a T_{trans} being T_m , is used as the molecular switching unit providing shape fixity. The chemically crosslinked PE network memorises the permanent shape after deformation upon heating (12, 36, 37), and the mechanism of the thermally-induced shape-memory PE (SMPE) is depicted in **Figure 2**.

The associated modulus of elasticity is dictated by configurational entropy reduction that occurs with deformation of the constituent chains and is therefore often termed entropy elasticity. For $T > T_{trans}$ (T_g , T_m or other), polymer networks exhibit super-elasticity wherein the polymer chain segments between crosslink points can deform quite freely and are prone to being twisted randomly *via* rotations about backbone bonds, maintaining a maximum entropy and minimum internal energy as macroscopic deformation occurs (12). The classic prediction from rubber

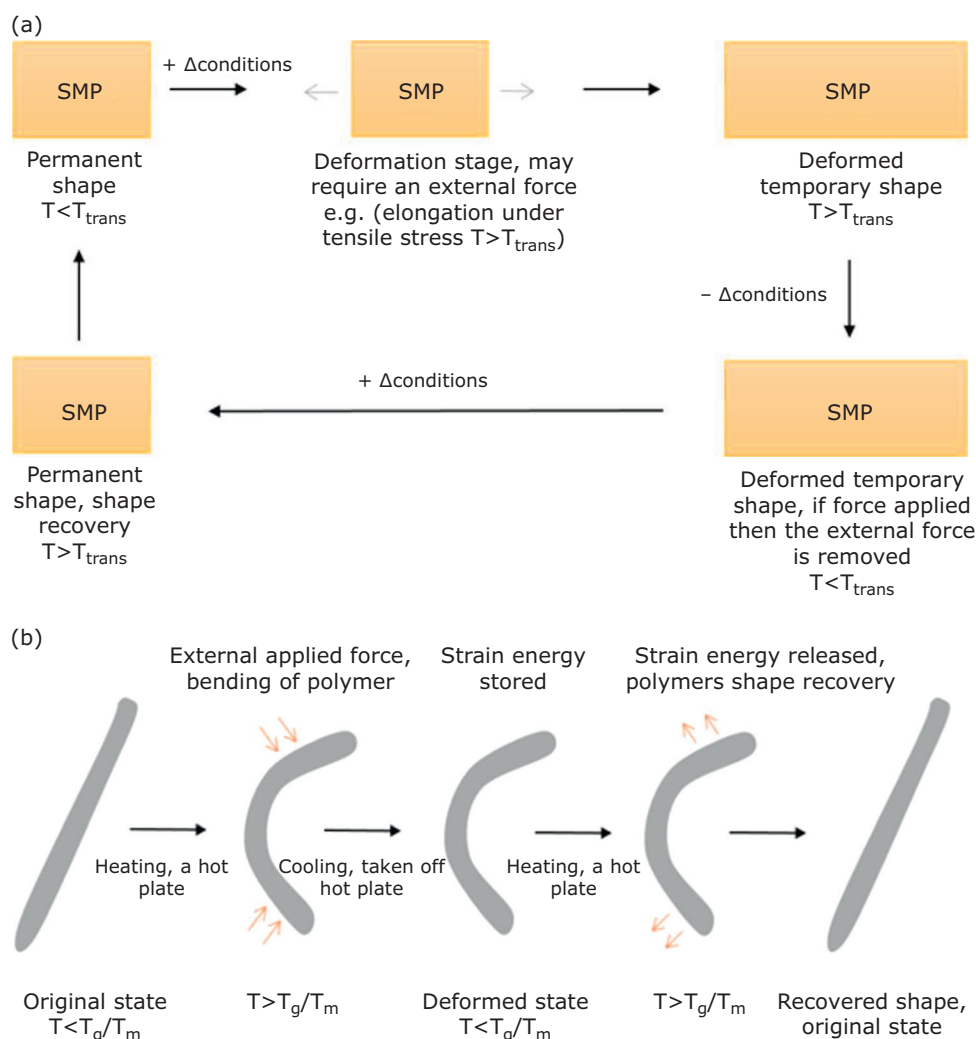


Fig. 1. (a) The general SME mechanism of SMPs; (b) thermally-responsive SMP

elastic theory is that the resulting elastic shear modulus (G) is proportional to both crosslink density and temperature (Equation (iii)):

$$G = \nu K_B T = \frac{\rho R T}{M_C} \tag{iii}$$

where ν is the number density of network chains, ρ the mass density, R the universal gas constant and M_C the molecular weight between crosslinks. From a macroscopic viewpoint, the SME in SMPs can be graphically represented in three-dimensions (3D). Tensile strain vs. temperature and tensile stress (for example, elongation) is depicted in **Figure 3**.

Using the shape-memory strain-temperature-stress relationship description in **Figure 3**, the features of SMPs that allow for good shape-memory behaviour include: a sharp transition that can be used to quickly fix the temporary shape at

low temperature, and the ability to trigger shape recovery at high temperature; super-elasticity above T_{trans} that leads to the eventual shape recovery and avoids residual strain (permanent deformation); and complete and rapid fixing of the temporary shape by immobilising the polymeric chains without creep thereafter (12, 37). Thus far, the SME models describing how SMPs recover their original state prominently involve thermo-responsive SMPs. However, careful design of the polymers allows the opportunity for SMPs to possess different stimuli responses and applications.

Shape-Memory Polymer Triggers

A multitude of different triggers for SMEs and SMPs exist. However, an in-depth review is outside the scope of this mini-review, and therefore a few examples are highlighted below.

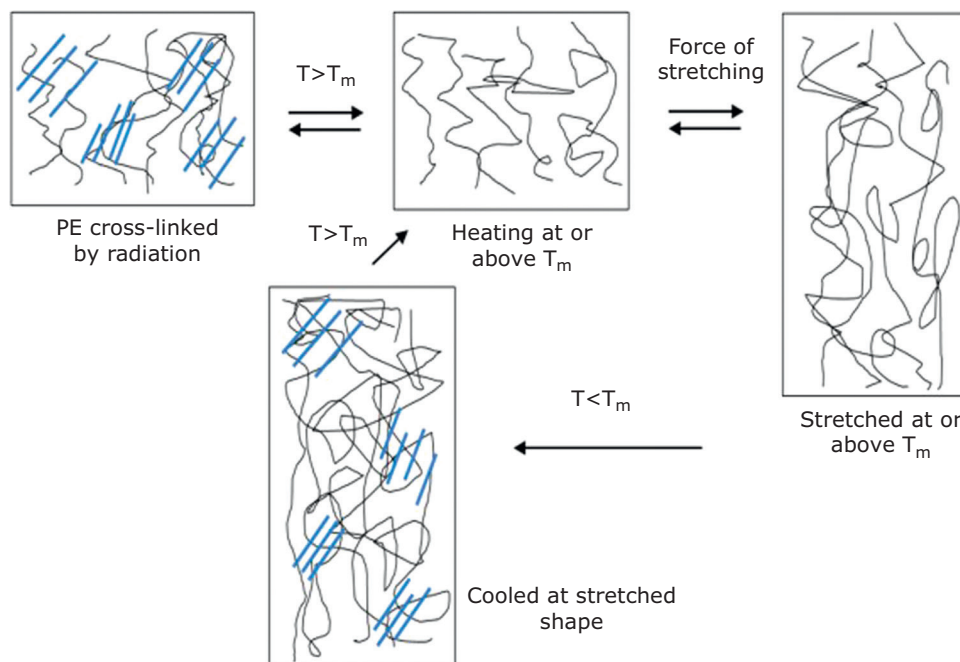


Fig. 2. Molecular model of the thermally-induced SME mechanism of crosslinked SMPE

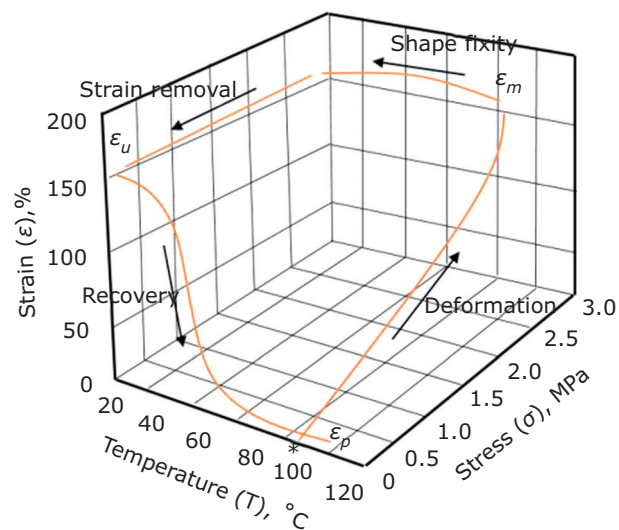


Fig. 3. A general 3D plot of an SMP during a thermomechanical shape-memory cycle

Thermally-Induced Shape-Memory Polymer

It is possible to generate thermally-induced SMEs in a variety of materials (18–20, 38–40), however a comprehensive overview is outside the scope of this mini-review. As previously discussed, the SME of SMPs can be thermally-induced, and these SMPs are the most common (26). **Figure 1** depicts a general overview of the SME mechanism of

SMPs, with a schematic of the SME mechanism for thermally-induced SMPs with T_g (amorphous cases) and T_m (crystalline cases). **Figure 2** presents a specific example of the SME mechanism for SMPE with the T_{trans} being T_m . In addition, advanced thermomechanical constitutive models have been used to study the materials’ behaviour (for example strain-temperature-stress development with time) in a very accurate way (41). By applying these models to SME mechanistic studies and the detailed characterisation of the SMPs (crosslinks, intermolecular and intramolecular interactions involving the SMPs) (12), a deeper understanding of the SME of SMPs can be achieved, which has proven beneficial for the development of new SMPs and their proposed applications (31). For example, poly(ϵ -caprolactone) (PCL), typically a biodegradable polymer, has been reported to possess high shape fixity and recovery. This was achieved by integrating reversible bonds within the PCL polymer network *via* the Diels-Alder addition of 1,2,4-triazoline-3,5-dione (TAD)-anthracene and Alder-ene addition of TAD-indole (42). These PCL SMPs were reported to attain recovery ratios greater than 99% (43). Furthermore, a dual-functional (self-healing and shape-memory) polymer network was achieved by crosslinking a polydimethylsiloxane (PDMS) polymer containing dense carboxylate groups (100% mol) (PDMS-COOH) with small amount of poly(ethylene glycol) diglycidyl ether

(PEGDGE) (44). This SMP (PDMS-COO-E) actuates at body temperature (37°C) with possible strain *ca.* 200% and shape recovery ratios at 98.06%. In addition, a 25 mm × 4 mm × 1 mm sample cut into two separate pieces healed (the two pieces become one whole piece with no evidence of a cut) when the two cut surfaces were brought into contact after 6 h at 25°C. Thus, the unique material, PDMS-COO-E, may have a wide range of applications in many fields, including wearable electronics, biomedical devices and four-dimensional (4D) printing (1, 19). Interestingly, the material was also reported to possess a greater than 85% light transmittance (425 nm to 700 nm) (44), therefore PDMS-COO-E has potential applications in transparent electronic devices. **Figure 4** illustrates the possible SME mechanism of PDMS-COO-E. The short PDMS linear chains are crosslinked by chemical covalent interactions and abundant hydrogen bonds into a 3D network. The covalent crosslinked networks of PDMS-COO-E maintain the permanent shape and resilience, whereas, at *ca.* 37°C the weak hydrogen bonds are broken, and the dynamics of polymer chains increase, resulting in recovering the permanent shape. Meanwhile, a large number of hydrogen bonds enable the samples to heal at temperature without external stimulus (44).

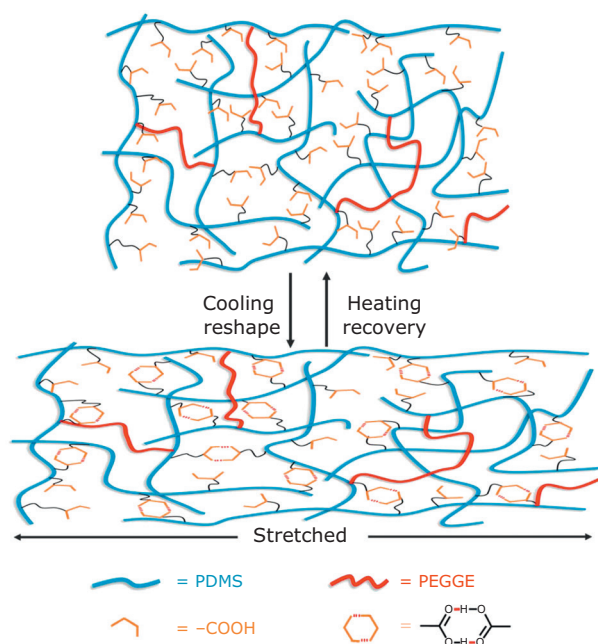


Fig. 4. The possible mechanism about shape memory effect of PDMS-COO-E polymer. Reprinted with permission from MDPI (44)

Light-Induced Shape-Memory Polymer

It is possible to generate light-induced SMEs in a variety of materials (18–20, 38, 40, 45), however a comprehensive overview is outside the scope of this mini-review. Light-activated SMPs (LASMPs) (46) typically use photothermal or photochemical (photocrosslinking or photocleavage) triggers for SMEs. For instance, photothermal LASMPs typically employ photo-absorber molecules and particles that convert light to heat, thereby increasing the temperature at the desired region within the LASMP. Photochemical LASMPs incorporate photosensitive molecules to create or cleave bonds during irradiation with light, imparting potentially very swift SMEs (47, 48). It is possible to improve the response time of SMPs by increasing the thermal conductivity with various conductive additives (49). However, the heating and cooling of materials with substantial thickness takes time, which can be minimised by using light to trigger transitions in LASMPs (46). It is also possible to generate multistimuli-responsive materials using components of the materials that respond to different wavelengths of light (for example, one wavelength of light to induce photocrosslinking, while a second wavelength of light cleaves bonds). It is possible to produce materials that can be reversibly switched between an elastomer and a rigid polymer employing polymers containing cinnamic groups (48) that can be fixed into pre-determined shapes utilising ultraviolet (UV) light illumination (>260 nm), and then recovered their original state when exposed to UV light at a different wavelength (<260 nm) (49). **Figure 5** depicts one example of the process of LASMPs shape recoverability.

Electrically-Induced Shape-Memory Polymer

It is possible to generate electrically-induced SMEs in a variety of materials (18, 20, 50–55), however a comprehensive overview is outside the scope of this mini-review. A variety of electrically conductive materials including organic electronic materials (including conductive polymers such as polypyrrole (PPy) (28, 56–58) and carbon nanotubes (CNTs) (59, 60)) and inorganic electronic materials (such as alloys, metals (61) and silver nanowires (NWs)), have been incorporated in materials displaying SMEs to impart swift triggers to the SMEs, enabling a variety of interesting applications.

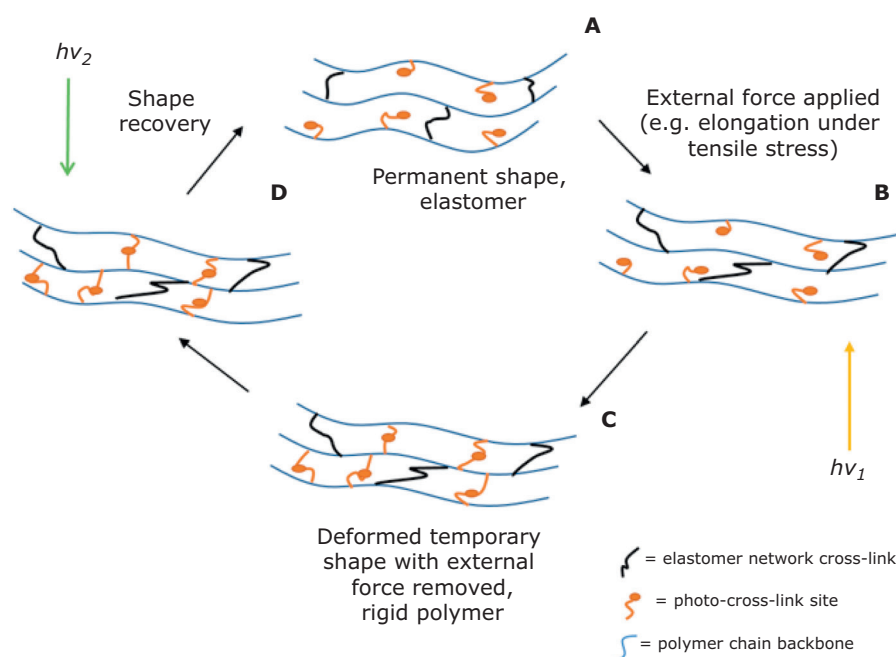


Fig. 5. Schematic of an example of the SME function of LASMPs

Highlighting some of the potential of electrically-induced SMEs, electrically-induced SMP composites incorporating shape-memory polyurethane (SMPU) and Ag NWs in a bilayer structure exhibits flexibility and electrical conductivity (62–64), which may find applications as capacitive sensors, healable transparent conductors and wearable electronics (65). In such materials the Ag NWs are randomly distributed on the surface layer of the composite to form a conductive percolating network that retains conductivity ($200 \Omega \text{ sq}^{-1}$) after a 12% elongation. However, continual increase in elongation causes a dramatic increase to the composites' resistance value and the eventual loss of electrical conductivity (66). When the material (deformed or in its original state), is connected to a typical circuit, a low voltage of 1.5 V was enough to activate a light-emitting diode (LED) (65). The composites possessing a higher Ag NW content exhibited a higher recovery ratio and reached the maximum recovery speed quicker (66). It was assumed that all the heat from electrical (Joule) heating was absorbed by the sample, i.e. no convective loss (67). Therefore, the composites with higher Ag NW content had a lower resistance value and the heating effectiveness was promoted. Heat initiates the thermal T_{trans} of the SMPU leading to an improved shape recovery, and voltages as low as 5 V reverted bent composites to their original state within 3 s (66). This represents a good example of a multifunctional SMP and demonstrates the potential

of SMP designs driving technological innovation. A schematic of the composite is shown in **Figure 6**.

Polymeric blend SMPs can be constructed from two immiscible polymeric matrices. The shape-recovery of these systems can be controlled with relative ease by varying the ratio of the polymer blends (68). However, this process may have adverse effects on shape-memory characteristics and diminish the material's performance, thereby limiting potential applications. On the other hand, SMP functionality may also be enhanced with other capabilities. For instance, it was recently reported that a new hybrid SMP was developed by combining single-walled CNTs (SWCNT) into a poly(lactic acid) (PLA) and thermoplastic polyurethane (TPU) SMP system, containing poly(ethylene glycol) (PEG) plasticiser (68). By incorporating PEG, the hybrid SMP composite achieved a lower temperature T_g (for example, 10 wt% of PEG lowered T_g of the PLA/TPU sample from 60°C to 40°C), meanwhile enhancing the dispersion of SWCNT (for instance, even at 4 wt% of SWCNT loading, 100% SMP tensile strain was possible, much greater than previously reported electrically-induced SMP studies, i.e. 12% discussed previously). In addition, the presence of the SWCNT can stabilise the SMP system and enhance its shape-fixity after deformations at room temperature conditions (68). Furthermore, the material was capable of a conductivity above $10^{-7} \text{ S cm}^{-1}$, which can be considered conductive, as documented (68). The PLA/TPU SMP composite (2 wt% SWCNT and

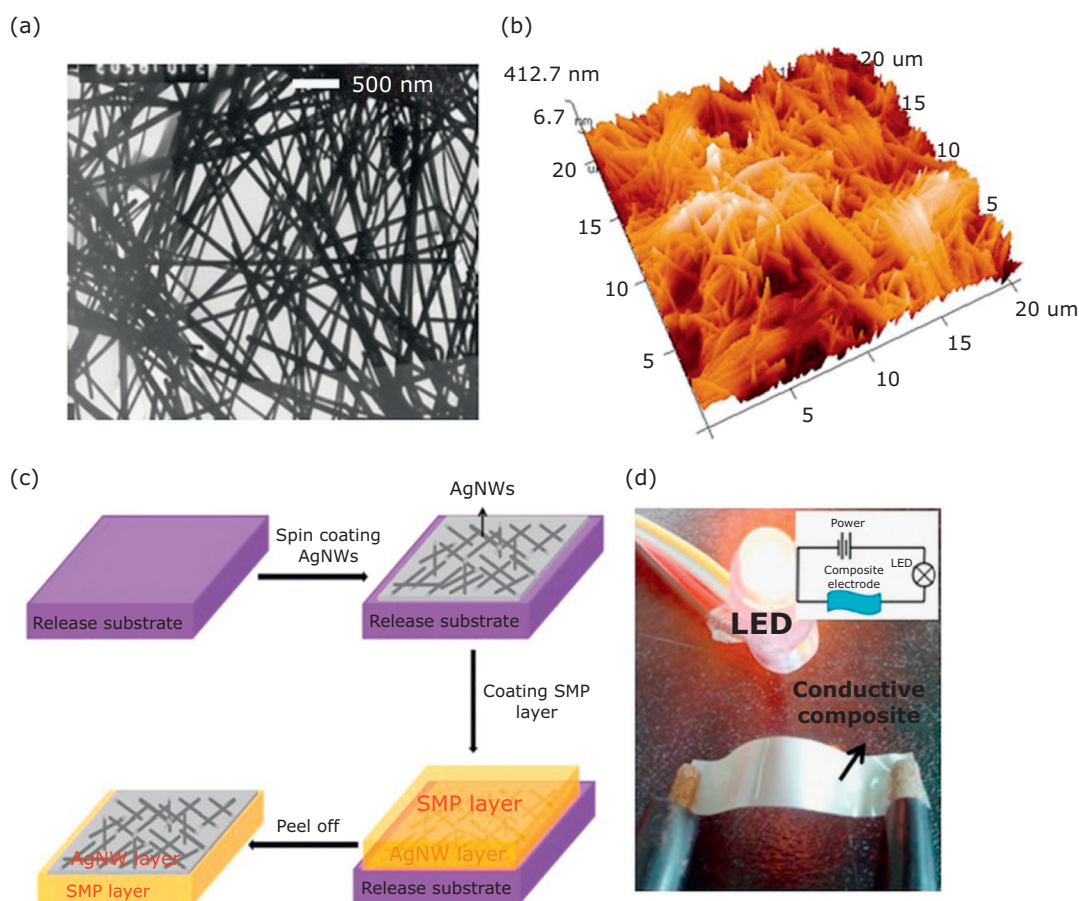


Fig. 6. (a) transmission electron microscopy (TEM) image of Ag NWs; (b) atomic force microscopy (AFM) image of Ag NWs; (c) schematic illustration of composites fabrication process; (d) the LED turned on as the composite was applied with voltages (the inset shows the circuit connecting with the composites). Reprinted with permission. Copyright 2014 Elsevier (66)

10 wt% PEG) also achieved shape-recovery, *via* Joule heating derived from electricity, in 80 s when currents of 125 mA were applied. The high stiffness of SWCNT filler results in decreasing shape-recovery performance because of the hindrance on the polymer chain movements (68). As a result, under room temperature stretching, the R_f and R_r values obtained were *ca.* 80% and 65%, respectively. Therefore, when its shape-recoverability is compared to other SMPs (shape-recovery ratios being upwards of 98%), the material is lacking. However, the hybrid SMP composite does possess electroactive ability, thus a trade-off relationship between shape-memory/recovery and electroactive ability needs to be carefully considered when designing similar materials.

Water-Induced Shape-Memory Polymer

It is possible to generate water-induced SMEs in a variety of materials (18, 20, 38, 39, 69–72),

however a comprehensive overview is outside the scope of this mini-review. Water is an important stimulus due to the fact it is abundant in a multitude of different environments, non-toxic and safe for a variety of applications.

An interesting example highlighting the potential of such materials is based on strong and flexible composite films (73) utilising the combination of a flexible interpenetrating polyol-borate network (74) and electroactive PPy (75, 76) that exchange water with the environment resulting in film expansion or contraction. The free-standing multi-functional SMP films were prepared by electropolymerisation of pyrrole in the presence of the polyol-borate complex (composed of pentaerythritol ethoxylate (PEE) coordinated to boron(III)) (74), wherein the interpenetrating network enables water-gradient-induced displacement, converting chemical potential energy in water gradients to mechanical work (73), and results in adaptation of the

architecture in response to an environmental condition change (i.e. sorption and desorption of water which drives the SME process, as depicted in **Figure 7**). The design of the water-responsive PPy-PEE composites was creatively applied to prepare actuators and generators driven by water gradients. The film actuator can generate contractile stress up to 27 MPa, lift objects 380 times heavier than itself and transport cargo 10 times heavier than itself (73). An assembled generator associating the actuator with a piezoelectric element driven by water gradients, outputs alternating electricity at *ca.* 0.3 Hz, with a peak voltage of *ca.* 1 V (73). The electrical energy can be stored in capacitors that could power micro and nanoelectronic devices (73). The SME mechanism for this SMP differs to that of **Figure 1** and **Figure 2**, utilising water as the shape-memory trigger for T_{trans} , and the original and deformed state interchange automatically *via* water sorption and desorption states. However, the shape-memory phenomenon remains the same, further demonstrating the potential of SMP designs driving technological innovation.

pH-Induced Shape-Memory Polymer

It is possible to generate pH-induced SMEs in a variety of materials (18, 20, 38, 77–80), however a comprehensive overview is outside the scope of this mini-review. An example of the interesting properties of such pH-responsive SMPs and their composites is produced by blending poly(ethylene glycol)-poly(ϵ -caprolactone)-based polyurethane (PECU) with functionalised cellulose nanocrystals (CNCs) displaying pH responsive pyridine moieties (CNC-C₆H₄NO₂) (81, 82). At high pH values the pyridine is deprotonated, facilitating hydrogen bonding interactions between the pyridine groups and hydroxyl moieties on the cellulose, whereas at low pH values, the protonation of the pyridine moieties diminishes these interactions. By comparison, carboxylic acid functionalised cellulose nanocrystals (CNC-CO₂H) responded to pH variation in the opposite manner (83–85). When the functionalised CNCs were combined with PECU polymer matrix to form a nanocomposite network, the mechanical properties of PECU were improved along with the pH-responsiveness of CNCs (85).

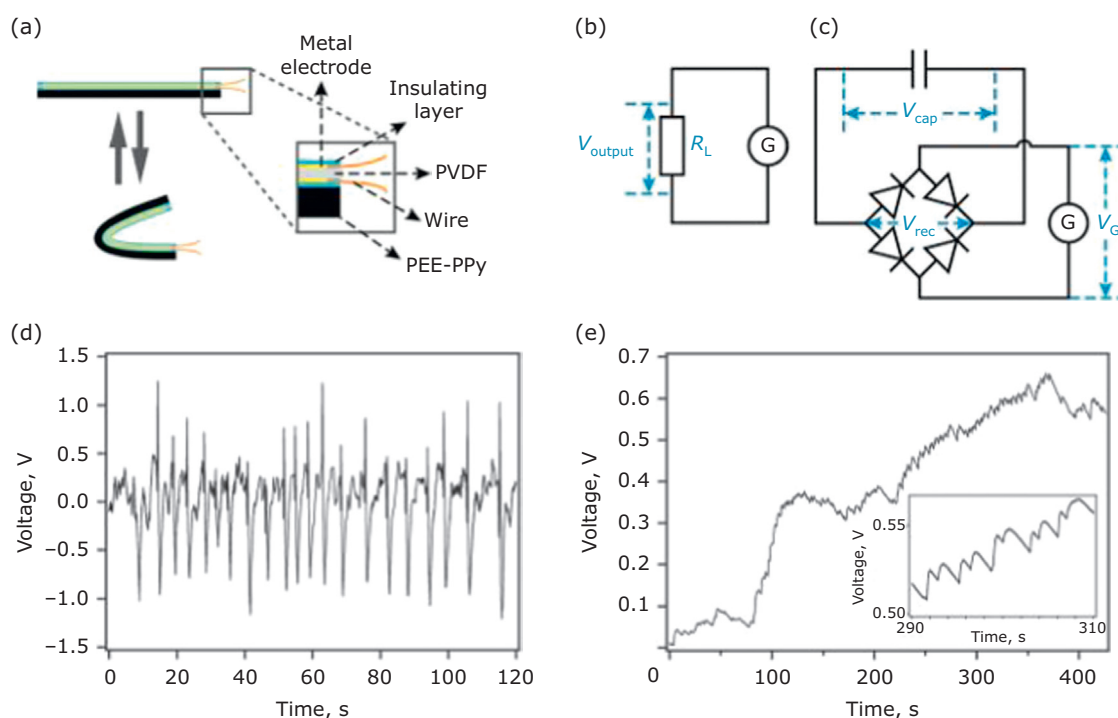


Fig. 7. Design and performance of a water-gradient-driven generator: (a) the assembly of a piezoelectric polyvinylidene fluoride (PVDF) element with a PEE-PPy actuator to form the generator; (b) the connection of the generator with a 10 MW resistor as load; (c) the configuration of the rectifying circuit and charge storage capacitor; (d) the generator's output voltage onto the 10 MW resistor; (e) voltage across a capacitor when being charged by the generator. The inset shows a stepwise increase in the capacitor voltage accompanying each cycle of the energy conversion process. Reprinted with permission. Copyright 2013 The American Association for the Advancement of Science (73)

The percolated network of pH-sensitive CNC in the polymer matrix served as the switching units for the shape-memory composite, the SME process of this material is depicted in **Figure 8** (81, 82). The CNC serves as the switching unit of the SMP composite within the matrix of PECU which is physically crosslinked and microphase separated to yield the net points. Such pH-responsive shape-memory nanocomposites have promise in the design of biomaterials for biomedical applications (for example, SMP-based drug delivery systems

triggered by transition along the digestive tract) (83).

Magnetically-Induced Shape-Memory Polymer

It is possible to generate magnetically-induced SMEs in a variety of materials (18, 20, 38, 86–88), however a comprehensive overview is outside the scope of this mini-review. The SMP devices discussed thus far are being researched with potential application into wearable electronics, nanoelectronics (such as actuators), biomaterials and biomedical devices (1, 18, 19). However, in some instances (such as medical devices) a key challenge is the design and implementation of a safe and effective method of actuating a variety of device geometries *in vivo*. As previously discussed, a pH-triggered SMP design can be potentially effective when utilised as drug delivery devices, when the target environment has a substantial pH difference (for instance, the digestive system) (83). However, the development of electrically and thermally-triggered devices that safely operate *in vivo* is difficult due to the (generally) high temperatures these SMPs can reach (relative to biological systems). For instance, the electroactive PLA-TPU SMP composite (2 wt% SWCNT and 10 wt% PEG) reaches temperatures greater than 70°C in 80 s as shape-recovery is achieved (68).

An alternative method of achieving actuation is inductive heating by loading ferromagnetic particles into an SMP system and exposing the doped device to an alternating electromagnetic field (89), benefiting from the innate thermoregulation offered by a ferromagnetic material's Curie temperature (T_c , at which a ferromagnetic material becomes paramagnetic, losing its ability to generate heat *via* a hysteresis loss mechanism) (90). By using particle sizes and materials that will heat mainly *via* a magnetic hysteresis loss mechanism over an eddy current mechanism, it is possible to have an innate thermoregulation mechanism that limits the maximum achievable temperature to T_c (89). Therefore, by selecting ferromagnetic particle materials with a T_c within safe medical limits, Curie thermoregulation eliminates the danger of overheating and the need for a feedback system to monitor implanted device temperatures (89). However, this technology is not only useful when applied to medical devices. Other useful applications include remote activation in which wires or connections to SMP devices could be eliminated, simplifying the design and reducing possible points

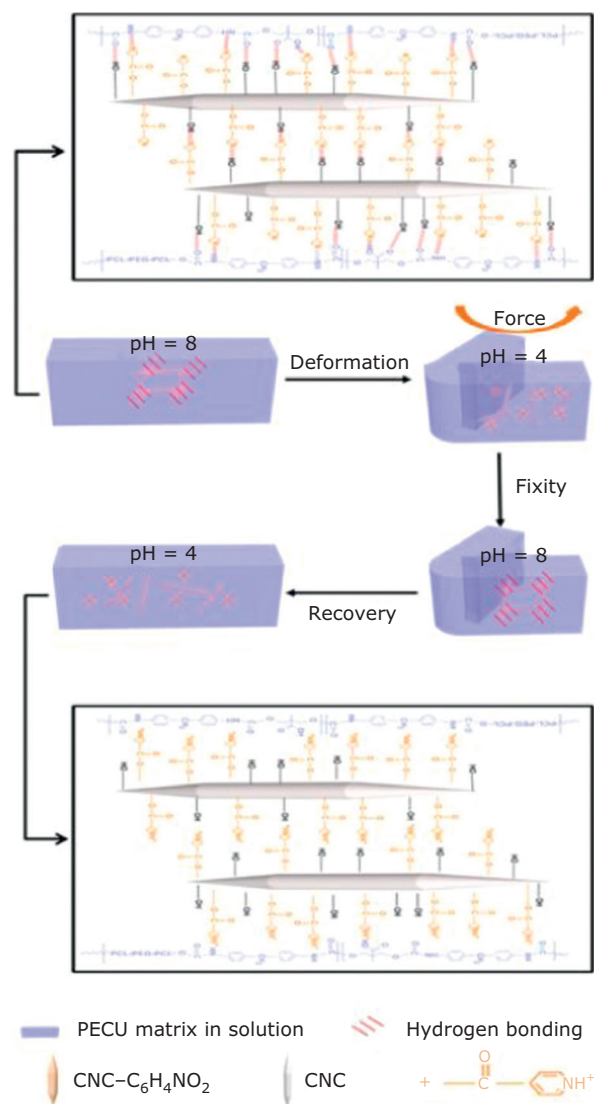


Fig. 8. Schematic representation of the pH-responsive shape-memory materials, which rely on hydrogen bonding switching mechanism in the interactions between cellulose nanocrystals (CNC-C₆H₄NO₂) within polymer matrix upon immersion in hydrochloric acid solution (pH = 4) or sodium hydroxide solution (pH = 8). Reprinted with permission. Copyright 2015 American Chemical Society (81)

of failure. An example of this method of actuation involves the incorporation of 10% by volume nickel zinc ferrites (for example C2050 (Ceramic Magnetics Inc, USA) and CMD5005 (Ceramic Magnetics Inc), particle sizes *ca.* 50 μm with spherical shapes) with an ester-based thermoset polyurethane (PU) SMP, MP5510 (SMP Technologies Inc, Japan) (T_g of 55°C) (89). The magnetic field utilised to achieve shape-recovery was a copper-wound solenoid coil with a 2.54 cm diameter, 7.62 cm length and with a total of 7.5 turns. The unit possessed an adjustable power setting capable of outputting 27 W to 1500 W at between 10 MHz and 15 MHz frequency (note: this high frequency may induce eddy currents in the tissue, causing undesirable direct heating of the human body in medical applications) (91). However, an alternating magnetic field of 12.2 MHz and approx. 400 A m^{-1} (centre of the inductive coil) at room temperature was used for actuation to demonstrate proof of concept for the device. It was also reported that clinically useable frequencies (50 kHz to 100 kHz) (92) should still be effective (89), albeit this could result at a different quantitative level (i.e. shape-recovery and memory performance may be reduced). Furthermore, C2050 and CMD5005 possess a T_c of 340°C and 130°C, respectively. These temperatures exceed physiological limits and are therefore not practical for medical devices currently, however, these doped SMP

composites did not exceed temperatures above the respective Ni Zn particle T_c values, signifying a thermoregulation characteristic. In addition, it was stated that the 10% volume of Ni Zn particles did not impact the SMPs shape-memory properties significantly (89). The T_g increased from 55°C to 61.4°C and the shape-recovery of a flower and foam-based device was achieved within 15 s to 25 s, at a temperature range of 23°C to 78.6°C. The potential applications for this device are illustrated in **Figure 9**. Optimisation of this device/design is still required before it can be considered clinically viable, however, this SMP composite highlights very interesting characteristics, remote activation (*via* magnetic fields inducing thermally-triggered actuation) and thermoregulation (*via* T_c temperature of the material being employed).

Shape-Memory Polymer Classification

As highlighted above, SMP materials are diverse and respond to many different external stimuli (including temperature, light, electricity, water, pH and electromagnetic fields) by a variety of mechanisms. Although SMPs can be classified based on their composition and structure, stimulus and shape-memory function, their classification can be difficult, as organising these polymeric smart materials into one or two simple categories

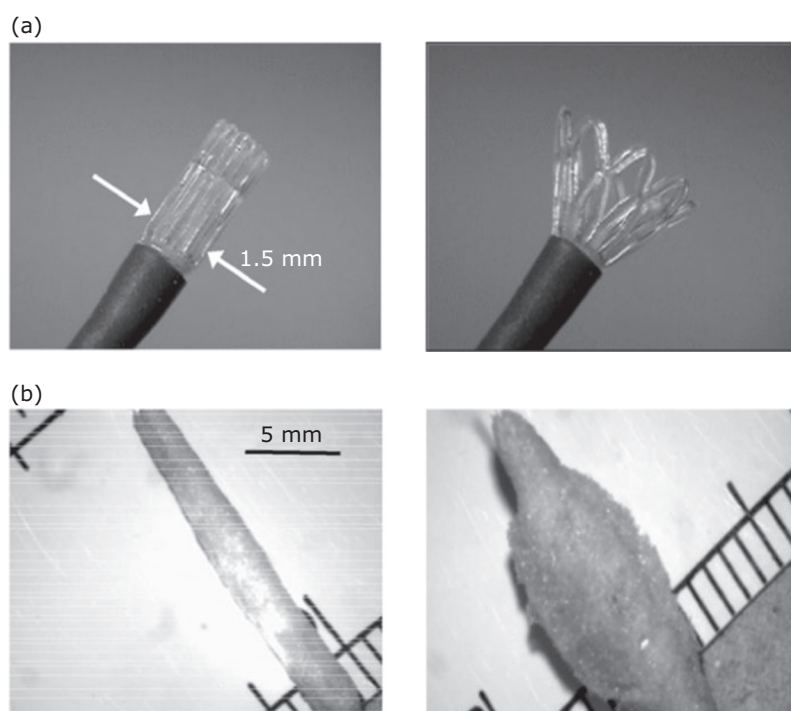


Fig. 9. SMP devices used to evaluate feasibility of actuation by inductive heating: (a) flower shaped device shown in collapsed and actuated form; (b) SMP foam device shown in collapsed and actuated form. Reproduced with permission. Copyright 2006 IEEE Transactions on Biomedical Engineering (89)

is an over-simplification of their abilities and characteristics (93).

SMPs are considered to consist of net points and molecular switches or stimuli sensitive domains. These net points can be achieved by covalent bonds (chemically crosslinked) or intermolecular interactions (physically crosslinked). Chemically crosslinked SMPs involve suitable crosslinking chemistry and are referred to as thermosets (94, 95). Physically crosslinked SMPs involve a polymer morphology consisting of at least two segregated domains and are referred to as thermoplastics (96). The network chains of the SMP can be either amorphous or crystalline and therefore, the T_{trans} is either a T_g or T_m . The network architectures are thought to be constructed through crosslinking net points, with polymer segments connecting adjacent net points. The strongly crosslinked architectures ensure the polymer can maintain a stable shape on the macroscopic level (93). Thermoplastic polymers exhibit a more reversible nature (97), meaning the physical crosslinked net points can be disrupted and reformed with relative ease. The interconnection of the individual polymer chains in a physically crosslinked network is achieved by the formation of crystalline or glassy phases. For thermoset polymers, the individual polymer chains are connected by covalent bonds and are therefore more stable than physically crosslinking networks and show an irreversible nature (98–100).

Regarding thermo-responsive SMPs, they can be classified according to the nature of their permanent net points and the T_{trans} related to the switching domains into four different categories: (a) physically crosslinked thermoplastics, $T_{\text{trans}} = T_g$; (b) physically crosslinked thermoplastics, $T_{\text{trans}} = T_m$; (c) chemically crosslinked amorphous polymers, $T_{\text{trans}} = T_g$; (d) chemically crosslinked semi-crystalline polymer networks $T_{\text{trans}} = T_m$ (93).

Thermoplastic Shape-Memory Polymers

For the physically crosslinked SMPs, the formation of a phase-segregated morphology is the fundamental mechanism behind the thermally-induced SME of these materials (93, 99). One phase provides the physical crosslinks while the other acts as a molecular switch. They can be further classified into linear polymers, branched polymers or a polymer complex. Linear SMPs may consist of block copolymers and high molecular weight polymers, the typical physically crosslinked SMP is linear block copolymers, such as PU. In

polyesterurethanes (PEU), oligourethane segments are the hard-elastic segments, while polyester serves as the switching segment (99).

Thermoset Shape-Memory Polymers

For chemically crosslinked SMPs, two methods are commonly used to synthesise covalently crosslinked networks (36, 41). The first method relies on addition of a multi-functional crosslinker during polymerisation (41), whereas the second method relies on the subsequent crosslinking of a linear or branched polymer (36). The networks are formed based on many different polymer backbones. Covalently crosslinked SMPs possess chemically interconnected structures determining the original macroscopic shape. The switching segments of these materials are generally the network chains between net points, and a T_{trans} of the polymer segments is used as the shape-memory switch. The chemical, thermal, mechanical and shape-memory properties are determined by the reaction conditions, curing times, the type and length of the network chains and the crosslinking density (35). Comparing physically crosslinked SMPs with chemically crosslinked SMPs, the chemically crosslinked SMPs often show less creep, thus, any irreversible deformation of the polymer during shape recovery is less. This is because covalent crosslinked networks are more stable than physical crosslinked networks. As a result, chemically crosslinked SMPs usually show better chemical, thermal, mechanical and shape-memory properties than physically crosslinked SMPs (96). For example, the shape recovery ratio of thermoplastic SMPU is usually in the range of 90% to 95% within 20 shape recovery cycles, and the elastic modulus is between 0.5 GPa and 2.5 GPa at room temperature (26). Additionally, when exposed to air, it is sensitive to moisture and therefore possesses unstable mechanical properties. In contrast, an epoxy SMP shows better overall performance as a shape-memory material. The shape recovery ratio typically reaches 98–100%, the elastic modulus between 2 GPa and 4.5 GPa, and it is generally stable in the presence of moisture (26). Thermoplastic SMPs (such as SMPU) are mostly researched and used as functional materials at a small scale, such as for biomaterials (30, 97). However, thermosetting SMPs (for example styrene-based SMP (SSMP) and epoxy SMPs) are generally used for structural materials, such as space deployable structures and automobile actuators (97, 98).

Shape-Memory Functionality

The approaches to designing different shape-memory functions become more abundant as scientists and engineers better understand the SME mechanism of SMPs. For instance, discussed thus far are examples of SMPs with polymeric blends, addition of crosslinking species, incorporation of electroactive and ferromagnetic substances. All of which enhances an SMP device functionality, enabling unique and interesting characteristics which can be tailored to a plethora of applications (for example, self-healing and wearable electronics, drug delivery and implantable medical devices) (101–110). Further still, one-way SMEs, two-way SMEs (such as dual shape PPy-PEE, discussed previously), triple SMEs, multiple SMEs and even temperature-memory effects (TMEs) have been widely investigated in SMPs (34). As the types of SMP materials increasingly diversify, two and even three different types of shape-memory functions can be achieved simultaneously in the same SMP material (34, 111). These types of materials can usually be achieved when combining different SMPs possessing different properties. A schematic of one-way, two-way, dual shape and triple shape functionality SMPs is shown in

Figure 10, and an integrated insight into the classification of SMPs is shown in **Figure 11**.

An example of a selective triple shape multicomposite SMP was documented to incorporate a neat SSMP (112) and two SSMP composites (113). One incorporated iron(II, III) oxide nanoparticles while the other CNT nanoparticles. This unique SMP composite successfully possessed three different regions within the sample: neat SSMP, SSMP-Fe₃O₄ and SSMP-CNT. Because of this, the material also possessed distinct shape-memory capabilities with different triggers. For instance, the material was documented undergoing a three-step shape-memory recovery process, subjected to an alternating magnetic field of 30 kHz, a radio frequency (RF) field of 13.56 MHz and direct oven heating at 130°C (113). Furthermore, the R_f and R_r for the original shape to the first temporary shape (and back to the original shape) was reported at 93% and 93%, respectively. Meanwhile, the R_f and R_r for the first temporary shape to the second temporary shape (and back to the first temporary shape) was at 95% and 99%, respectively (113). The SME mechanism for this multicomposite is represented in **Figure 12** and it was concluded that this unique material has promising characteristics to be used in biomimetic materials. Examples of

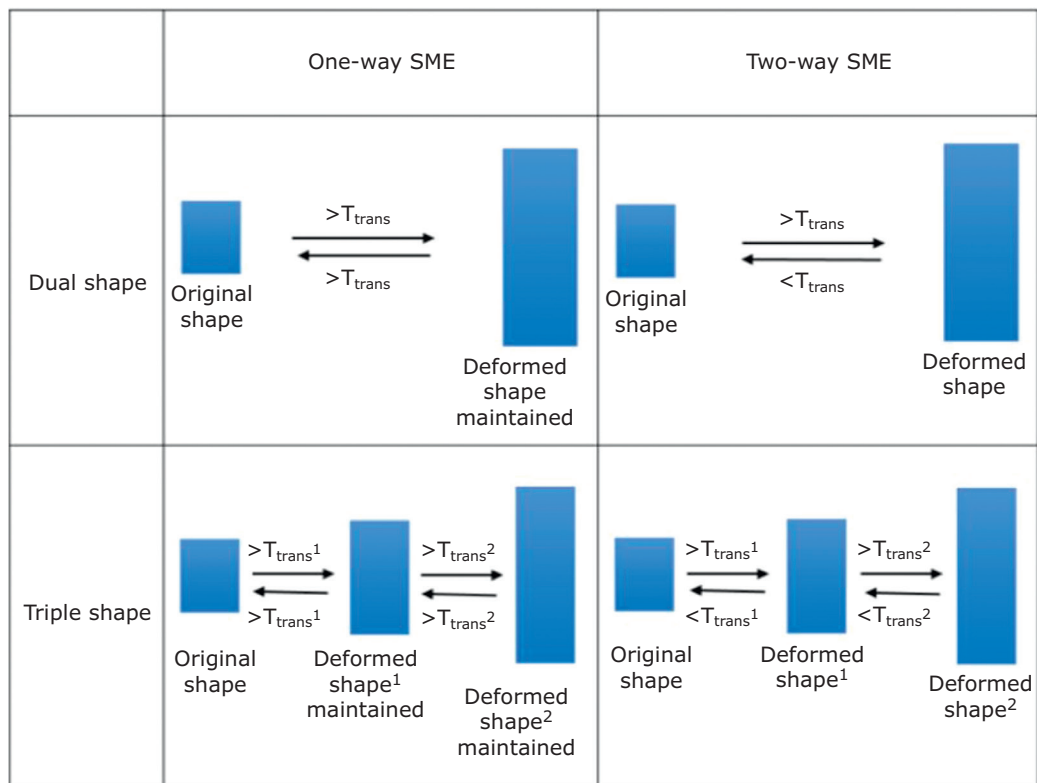


Fig. 10. The varying shape-memory functionality of SMPs

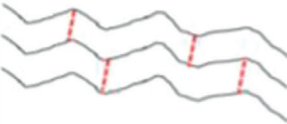
Composition and structure	Stimulus	Shape-memory function type
Block copolymer 	TEMPERATURE	ONE-WAY SME
	ELECTRICITY	
Supramolecular polymer		MAGNETIC
		
Polymer blend/composites e.g. PPy-PEE discussed in Figure 7 	WATER SENSITIVE	TRIPLE SHAPE SME
Cross-linked homopolymer 	OXIDATION-REDUCTION	MULTI-SHAPE SME
Polymer IPN/semi-IPN 	LIGHT/RADIATION	MULTI-FUNCTIONALITY

Fig. 11. The classification of SMPs based on composition and structure, stimulus triggers and the possible type of shape-memory functions

applications of SMP-based materials and their composites are highlighted in **Table I**.

Conclusion

As the understanding of SMPs continually develops among the academic and industrial communities, the generation of new and potentially innovative SMPs will be more rapid while we realise the full potential of these materials. SMPs are one of the most interesting of polymer classes within the field of functional polymers. In addition, SMP composites can enhance the already impressive capabilities of

SMPs by imparting new functional characteristics, broadening the potential applications of these materials and enabling a multipurpose material. SMPs and their composites are capable of industrially important applications (examples of which include: self-healing (101–104), generators driven by water gradients (73), sensors (72), task-specific medical devices (18, 105) and wearable electronics (106–110), a few examples of which are highlighted in **Table I**. The literature published to date de-risks investment from governments and industry to raise the technology readiness levels towards products on the market.

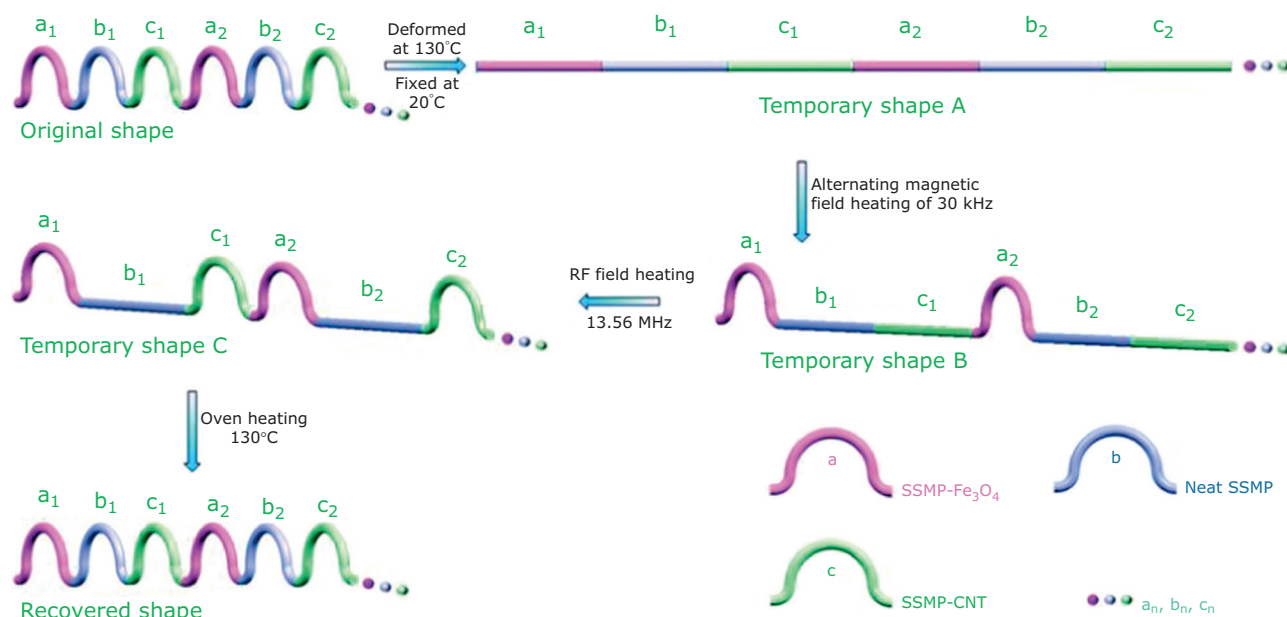


Fig. 12. Schematic of the selective shape recoveries of the multicomposite SSMP induced by alternating magnetic field heating, RF field heating and oven heating, respectively (a_n , b_n and c_n stand for the n sections of SSMP- Fe_3O_4 , neat SSMP and SSMP-CNT, respectively). Reproduced by permission of The Royal Society of Chemistry. Copyright 2015 The Royal Society of Chemistry (113)

Table I Examples of Applications of SMP-Based Materials and Their Composites

Application	References
Actuators (for example, for generators)	(73)
Biomedical devices (such as drug delivery systems, expanding foam and endovascular thrombectomy device)	(44, 83, 89)
Multipurpose/multifunctionality (for example, self-healing, biocompatible, body temperature actuation and selective triple shape-memory)	(44, 113)
Thermoregulators	(89, 90)
Wearable electronics	(65, 68)

Acknowledgements

We acknowledge the Faculty of Science and Technology, Lancaster University, UK, for an Early Career Internal Grant and The Royal Society, UK, for a Research Grant (RG160449). We acknowledge the Engineering and Physical Sciences Research Council (EPSRC), UK, for an EPSRC First Grant (EP/R003823/1) and a Pathfinder Grant from the EPSRC Centre for Innovative Manufacturing in Large Area Electronics (EP/K03099X/1). We also thank the Biotechnology and Biological Sciences Research Council (BBSRC), UK, for financial support of

research aligned with some of the topics discussed in this review, specifically the Glycoscience Tools for Biotechnology and Bioenergy (IBCarb) Network in Industrial Biotechnology and Bioenergy (NIBB, BB/L013762/1); the BBSRC FoodWasteNet NIBB (BB/L0137971/1), the BBSRC From Plants to Products (P2P) NIBB (BB/L013819/1) and the Lignocellulosic Biorefinery Network (LBNNet) NIBB (BB/L013738/1).

References

1. A. Lendlein and O. E. C. Gould, *Nat. Rev. Mater.*, 2019, 4, (2), 116

2. T. Biggs, M. B. Cortie, M. J. Witcomb and L. A. Cornish, *Platinum Metals Rev.*, 2003, **47**, (4), 142
3. D. Kapoor, *Johnson Matthey Technol. Rev.*, 2017, **61**, (1), 66
4. Y. V. Kudriavtsev and E. L. Semenova, *Platinum Metals Rev.*, 2014, **58**, (1), 20
5. R. Oshima, S. Muto and T. Hamada, *Platinum Metals Rev.*, 1988, **32**, (3), 110
6. J. M. Jani, M. Leary, A. Subic and M. A. Gibson, *Mater. Des.*, 2014, **56**, 1078
7. C. Naresh, P. S. C. Bose and C. S. P. Rao, 'Shape Memory Alloys: A State of Art Review', International Conference on Advances in Materials and Manufacturing Applications (IConAMMA-2016), Bangalore, India, 14th–16th July, 2016, IOP Conference Series: Materials Science and Engineering, Vol. 149, IOP Publishing Ltd, Bristol, UK, 2016
8. D. Patil and G. Song, *Smart Mater. Struct.*, 2017, **26**, (9), 093002
9. N. Ma, Y. Lu, J. He and H. Dai, *J. Text. Inst.*, 2019, **110**, (6), 950
10. C. Wen, X. Yu, W. Zeng, S. Zhao, L. Wang, G. Wan, S. Huang, H. Grover and Z. Chen, *AIMS Mater. Sci.*, 2018, **5**, (4), 559
11. W. M. Huang, Z. Ding, C. C. Wang, J. Wei, Y. Zhao and H. Purnawali, *Mater. Today*, 2010, **13**, (7–8), 54
12. C. Liu, H. Qin and P. T. Mather, *J. Mater. Chem.*, 2007, **17**, (16), 1543
13. Y. Liu, H. Du, L. Liu and J. Leng, *Smart Mater. Struct.*, 2014, **23**, (2), 023001
14. W. Sokolowski, A. Metcalfe, S. Hayashi, L. Yahia and J. Raymond, *Biomed. Mater.*, 2007, **2**, (1), S23
15. P. K. Kumar and D. C. Lagoudas, 'Introduction to Shape Memory Alloys', in "Shape Memory Alloys", ed. D. C. Lagoudas, Springer, Boston, USA, 2008, pp. 1–51
16. K. Yu, T. Xie, J. Leng, Y. Ding and H. J. Qi, *Soft Matter*, 2012, **8**, (20), 5687
17. J. G. Hardy, M. Palma, S. J. Wind and M. J. Biggs, *Adv. Mater.*, 2016, **28**, (27), 5717
18. K. Wang, S. Strandman and X. X. Zhu, *Front. Chem. Sci. Eng.*, 2017, **11**, 143
19. M. Behl and A. Lendlein, *Mater. Today*, 2007, **10**, (4), 20
20. H. Meng and G. Li, *Polymer*, 2013, **54**, (9), 2199
21. L. Sun, W. M. Huang, Z. Ding, Y. Zhao, C. C. Wang, H. Purnawali and C. Tang, *Mater. Des.*, 2012, **33**, 577
22. I. Bellin, S. Kelch, R. Langer and A. Lendlein, *Proc. Natl. Acad. Sci.*, 2006, **103**, (48), 18043
23. F. Pilate, A. Toncheva, P. Dubois and J.-M. Raquez, *Eur. Polym. J.*, 2016, **80**, 268
24. F. Ji, Y. Zhu, J. Hu, Y. Liu, L.-Y. Yeung and G. Ye, *Smart Mater. Struct.*, 2006, **15**, (6), 1547
25. R. Mohr, K. Kratz, T. Weigel, M. Lucka-Gabor, M. Moneke and A. Lendlein, *Proc. Natl. Acad. Sci.*, 2006, **103**, (10), 3540
26. J. Leng, X. Lan, Y. Liu and S. Du, *Prog. Mater. Sci.*, 2011, **56**, (7), 1077
27. B. Yang, W. M. Huang, C. Li and L. Li, *Polymer*, 2006, **47**, (4), 1348
28. N. G. Sahoo, Y. C. Jung and J. W. Cho, *Mater. Manuf. Processes*, 2007, **22**, (4), 419
29. A. Lendlein, H. Jiang, O. Jünger and R. Langer, *Nature*, 2005, **434**, 879
30. A. Lendlein and R. Langer, *Science*, 2002, **296**, (5573), 1673
31. K. Inoue, M. Yamashiro and M. Iji, *J. Appl. Polym. Sci.*, 2009, **112**, (2), 876
32. L. B. Vernon and H. M. Vernon, The Vernon Benschoff Company, 'Process of Manufacturing Articles of Thermoplastic Synthetic Resins', *US Patent 2,234,993*; 1941
33. W. C. Rainer, E. M. Redding, J. J. Hitov, A. W. Sloan and W. D. Stewart, W. R. Grace & Co, 'Polyethylene Product and Process', *US Patent 3,144,398*; 1964
34. J. Hu, Y. Zhu, H. Huang and J. Lu, *Prog. Polym. Sci.*, 2012, **37**, (12), 1720
35. A. Lendlein and S. Kelch, *Angew. Chem. Int. Ed.*, 2002, **41**, (12), 2034
36. S. Ota, *Radiat. Phys. Chem.*, 1981, **18**, (1–2), 81
37. Q. Zhao, H. J. Qi and T. Xie, *Prog. Polym. Sci.*, 2015, **49–50**, 79
38. X. Wu, W. M. Huang, Y. Zhao, Z. Ding, C. Tang and J. Zhang, *Polymers*, 2013, **5**, (4), 1169
39. Y. Bai, J. Zhang and X. Chen, *ACS Appl. Mater. Interfaces*, 2018, **10**, (16), 14017
40. K. Yu, Y. Liu and J. Leng, *RSC Adv.*, 2014, **4**, (6), 2961
41. I. A. Rousseau and P. T. Mather, *J. Am. Chem. Soc.*, 2003, **125**, (50), 15300
42. J. Caprasse, T. Defize, R. Riva and C. Jérôme, 'Comparative Study of PCL Shape-Memory Networks with Diels-Alder or Alder-ene Adducts', Advanced Functional Polymers for Medicine (AFPM), Montpellier, France, 16th–18th May, 2018

43. T. Defize, R. Riva, J.-M. Raquez, P. Dubois, C. Jérôme and M. Alexandre, *Macromol. Rapid Commun.*, 2011, **32**, (16), 1264
44. H.-Y. Lai, H.-Q. Wang, J.-C. Lai and C.-H. Li, *Molecules*, 2019, **24**, (18), 3224
45. D. Iqbal and M. H. Samiullah, *Materials*, 2013, **6**, (1), 116
46. D. J. Maitland, M. F. Metzger, D. Schumann, A. Lee and T. S. Wilson, *Lasers Surg. Med.*, 2002, **30**, (1), 1
47. H. Xie, K.-K. Yang and Y.-Z. Wang, *Prog. Polym. Sci.*, 2019, **95**, 32
48. Z. Yuan, A. Muliana and K. R. Rajagopal, *Math. Mech. Solids*, 2016, **22**, (5), 1116
49. E. Havens, E. A. Snyder and T. H. Tong, 'Light-Activated Shape Memory Polymers and Associated Applications', SPIE Smart Structures and Materials + Nondestructive Evaluation and Health Monitoring, San Diego, California, USA, 5th May, 2005, "Smart Structures and Materials 2005: Industrial and Commercial Applications of Smart Structures Technologies", Vol. 5762, Society of Photo-Optical Instrumentation Engineers (SPIE), Bellingham, USA, 2005, 8 pp
50. Y. Liu, H. Lv, X. Lan, J. Leng and S. Du, *Compos. Sci. Technol.*, 2009, **69**, (13), 2064
51. H. Lu, Y. Yao and L. Lin, *Pigm. Resin Technol.*, 2014, **34**, (1), 26
52. J. Alam, A. Khan, M. Alam and R. Mohan, *Materials*, 2015, **8**, (9), 6391
53. J. Zhang, X. Ke, G. Gou, J. Seidel, B. Xiang, P. Yu, W.-I. Liang, A. M. Minor, Y. Chu, G. Van Tendeloo, X. Ren and R. Ramesh, *Nat. Commun.*, 2013, **4**, 2768
54. X. Gong, L. Liu, Y. Liu and J. Leng, *Smart Mater. Struct.*, 2016, **25**, (3), 035036
55. J. Zhou, H. Li, R. Tian, R. Dugnani, H. Lu, Y. Chen, Y. Guo, H. Duan and H. Liu, *Sci. Rep.*, 2017, **7**, 5535
56. S.-K. Lee, S.-J. Lee, H.-J. An, S.-E. Cha, J.-K. Chang, B. Kim and J. J. Pak, 'Biomedical Applications of Electroactive Polymers and Shape-Memory Alloys', SPIE's 9th Annual International Symposium on Smart Structures and Materials, San Diego, USA, 11th July, 2002, "Smart Structures and Materials 2002: Electroactive Polymer Actuators and Devices (EAPAD)", Vol. 4695, Society of Photo-Optical Instrumentation Engineers (SPIE), Bellingham, USA, 2002, 15 pp
57. N. G. Sahoo, Y. C. Jung, H. J. Yoo and J. W. Cho, *Compos. Sci. Technol.*, 2007, **67**, (9), 1920
58. N. G. Sahoo, Y. C. Jung, N. S. Goo and J. W. Cho, *Macromol. Mater. Eng.*, 2005, **290**, (11), 1049
59. G. Zhou, H. Zhang, S. Xu, X. Gui, H. Wei, J. Leng, N. Koratkar and J. Zhong, *Sci. Rep.*, 2016, **6**, 24148
60. M. Dahmardeh, M. S. M. Ali, T. Saleh, T. M. Hian, M. V. Moghaddam, A. Nojeh and K. Takahata, *Phys. Status Solidi A*, 2013, **210**, (4), 631
61. H. B. Gilbert and R. J. Webster, *IEEE Robot. Autom. Lett.*, 2016, **1**, (1), 98
62. M. Xie, L. Wang, J. Ge, B. Guo and P. X. Ma, *ACS Appl. Mater. Interfaces*, 2015, **7**, (12), 6772
63. H. Tanaka and K. Honda, *J. Polym. Sci. Pol. Chem.*, 1977, **15**, (11), 2685
64. H. Luo, J. Hu and Y. Zhu, *Mater. Letters*, 2012, **89**, 172
65. C. Gong, J. Liang, W. Hu, X. Niu, S. Ma, H. T. Hahn and Q. Pei, *Adv. Mater.*, 2013, **25**, (30), 4186
66. H. Luo, Z. Li, G. Yi, X. Zu, H. Wang, Y. Wang, H. Huang, J. Hu, Z. Liang and B. Zhong, *Mater. Letters*, 2014, **134**, 172
67. T. Akter and W. S. Kim, *ACS Appl. Mater. Interfaces*, 2012, **4**, (4), 1855
68. Y.-C. Sun, M. Chu, M. Huang, O. Hegazi and H. E. Naguib, *Macromol. Mater. Eng.*, 2019, **304**, (10), 1900196
69. Y. Guo, Z. Lv, Y. Huo, L. Sun, S. Chen, Z. Liu, C. He, X. Bi, X. Fan and Z. You, *J. Mater. Chem. B*, 2019, **7**, (1), 123
70. I. T. Garces, S. Aslanzadeh, Y. Boluk and C. Ayranci, *Materials*, 2019, **12**, (2), 244
71. K. Fan, W. M. Huang, C. C. Wang, Z. Ding, Y. Zhao, H. Purnawali, K.C. Liew and L. X. Zheng, *eXPRESS Polym. Lett.*, 2011, **5**, (5), 409
72. L. Sun, T. X. Wang, H. M. Chen, A. V. Salvekar, B. S. Naveen, Q. Xu, Y. Weng, X. Guo, Y. Chen and W. M. Huang, *Polymers*, 2019, **11**, (6), 1049
73. M. Ma, L. Guo, D. G. Anderson and R. Langer, *Science*, 2013, **339**, (6116), 186
74. M. Shibayama, M. Sato, Y. Kimura, H. Fujiwara and S. Nomura, *Polymer*, 1988, **29**, (2), 336
75. E. Smela, *Adv. Mater.*, 2003, **15**, (6), 481
76. R. H. Baughman, *Science*, 2005, **308**, (5718), 63
77. Q. Song, H. Chen, S. Zhou, K. Zhao, B. Wang and P. Hu, *Polym. Chem.*, 2016, **7**, (9), 1739
78. H. Xiao, C. Ma, X. Le, L. Wang, W. Lu, P. Theato, T. Hu, J. Zhang and T. Chen, *Polymers*, 2017, **9**, (4), 138
79. X.-J. Han, Z.-Q. Dong, M.-M. Fan, Y. Liu, J.-H. Li, Y.-F. Wang, Q.-J. Yuan, B.-J. Li and S. Zhang, *Macromol. Rapid Commun.*, 2012, **33**, (12), 1055
80. J. Li, Q. Duan, E. Zhang and J. Wang, *Adv. Mater. Sci. Eng.*, 2018, 7453698

81. Y. Li, H. Chen, D. Liu, W. Wang, Y. Liu and S. Zhou, *ACS Appl. Mater. Interfaces*, 2015, **7**, (23), 12988
82. T. Wu, Y. Su and B. Chen, *ChemPhysChem*, 2014, **15**, (13), 2794
83. H. Chen, Y. Li, Y. Liu, T. Gong, L. Wang and S. Zhou, *Polym. Chem.*, 2014, **5**, (17), 5168
84. K. H. M. Kan, J. Li, K. Wijesekera and E. D. Cranston, *Biomacromolecules*, 2013, **14**, (9), 3130
85. A. E. Way, L. Hsu, K. Shanmuganathan, C. Weder and S. J. Rowan, *ACS Macro. Lett.*, 2012, **1**, (8), 1001
86. N. Gabdullin and S. H. Khan, 'Review of Properties of Magnetic Shape Memory (MSM) Alloys and MSM Actuator Designs', 2014 Joint IMEKO TC1-TC7-TC13 Symposium: Measurement Science Behind Safety and Security, Madeira, Portugal, 3rd–5th September, 2014, Journal of Physics: Conference Series, Vol. 588, IOP Publishing Ltd, Bristol, UK, 2015, 6 pp
87. E. Faran and D. Shilo, *Exp. Tech.*, 2016, **40**, (3) 1005
88. J. Karger-Kocsis and S. Kéki, *Polymers*, 2018, **10**, (1), 34
89. P. R. Buckley, G. H. McKinley, T. S. Wilson, W. Small, W. J. Bennett, J. P. Bearinger, M. W. McElfresh and D. J. Maitland, *IEEE Trans. Biomed. Eng.*, 2006, **53**, (10), 2075
90. A. Goldman, "Modern Ferrite Technology", Springer Verlag, New York, USA, 2006
91. P. R. Stauffer, T. C. Cetas, A. M. Fletcher, D. W. Deyoung, M. W. Dewhirst, J. R. Oleson and R. B. Roemer, *IEEE Trans. Biomed. Eng.*, 1984, **BME-31**, (1), 76
92. A. Jordan, R. Scholz, P. Wust, H. Föhling and R. Felix, *J. Magn. Magn. Mater.*, 1999, **201**, (1–3), 413
93. X. Fu, Y. Yuan, Z. Liu, P. Yan, C. Zhou and J. Lei, *Eur. Polym. J.*, 2017, **93**, 307
94. A. M. Kushner, J. D. Vossler, G. A. Williams and Z. Guan, *J. Am. Chem. Soc.*, 2009, **131**, (25), 8766
95. A. Li, J. Fan and G. Li, *J. Mater. Chem. A*, 2018, **6**, (24), 11479
96. F. Xie, L. Huang, J. Leng and Y. Liu, *J. Intell. Mater. Syst. Struct.*, 2016, **27**, (18), 2433
97. S. Kelch, S. Steuer, A. M. Schmidt and A. Lendlein, *Biomacromolecules*, 2007, **8**, (3), 1018
98. J. Leng, H. Lu, Y. Liu, W. M. Huang and S. Du, *MRS Bull.*, 2009, **34**, (11), 848
99. B. K. Kim, S. Y. Lee and M. Xu, *Polymer*, 1996, **37**, (26), 5781
100. S. Rimdusit, M. Lohwerathama, K. Hemvichian, P. Kasemsiri and I. Dueramae, *Smart Mater. Struct.*, 2013, **22**, (7), 075033
101. H. Luo, H. Wang, H. Zhou, X. Zhou, J. Hu, G. Yi, Z. Hao and W. Lin, *Appl. Sci.*, 2018, **8**, (3), 392
102. J. Zhang, M. Huo, M. Li, T. Li, N. Li, J. Zhou and J. Jiang, *Polymer*, 2018, **134**, 35
103. G. Ji, P. Zhang, J. Nji, M. John and G. Li, '11 - Shape Memory Polymer-Based Self-Healing Composites', in "Recent Advances in Smart Self-healing Polymers and Composites", eds. G. Li and H. Meng, Woodhead Publishing Series in Composites Science and Engineering, ch. 11, Woodhead Publishing, Cambridge, UK, 2015, pp 293–363
104. A. V. Menon, G. Madras and S. Bose, *Polym. Chem.*, 2019, **10**, (32), 4370
105. A. Lendlein, M. Behl, B. Hiebl and C. Wischke, *Expert Rev. Med. Devices*, 2010, **7**, (3), 357
106. M. P. Gaj, A. Wei, C. Fuentes-Hernandez, Y. Zhang, R. Reit, W. Voit, S. R. Marder and B. Kippelen, *Org. Electron.*, 2015, **25**, 151
107. S. J. Park and C. H. Park, *Sci. Rep.*, 2019, **9**, 9157
108. S. Thakur 'Shape Memory Polymers for Smart Textile Applications', in "Textiles for Advanced Applications", eds. B. Kumar and S. Thakur, ch. 12, Intech, Rijeka, Croatia, 2017, 432 pp
109. L. Li, P. Shi, Li Hua, J. An, Y. Gong, R. Chen, C. Yu, W. Hua, F. Xiu, J. Zhou, G. Gao, Z. Jin, G. Sun and W. Huang, *Nanoscale*, 2018, **10**, (1), 118
110. Y. Huang, M. Zhu, Z. Pei, Q. Xue, Y. Huang and C. Zhi, *J. Mater. Chem. A*, 2016, **4**, (4), 1290
111. S. Ahn, P. Deshmukh and R. M. Kasi, *Macromolecules*, 2010, **43**, (17), 7330
112. J. Leng, D. Zhang, Y. Liu, K. Yu and X. Lan, *Appl. Phys. Lett.*, 2010, **96**, 111905
113. W. Li, Y. Liu and J. Leng, *J. Mater. Chem. A*, 2015, **3**, (48), 24532

The Authors



Mathew John Haskew received his BSc in Chemistry from Lancaster University, UK, and subsequently undertook an MSc by research on SMP-based materials (with John Hardy at Lancaster University). He is currently undertaking a PhD in Engineering with Samuel Murphy and John Hardy at Lancaster University. His PhD involves the development of biodegradable biomaterials, and a combination of computational modelling and experimental validation of their efficacy.



John George Hardy received his MSci and PhD in Chemistry from the University of Bristol, UK, and the University of York, UK, respectively. Thereafter he undertook postdoctoral research in Biochemistry, Biomedical Engineering, Materials Science and Pharmacy (in France, Germany, Northern Ireland and the USA) before returning to the UK to lead a research group developing stimuli-responsive materials for technical and medical applications.